

Periphyton as an indicator of saltwater intrusion into freshwater wetlands: insights from experimental manipulations

VIVIANA MAZZEI ,¹ BENJAMIN J. WILSON , SHELBY SERVAIS, SEAN P. CHARLES, JOHN S. KOMINOSKI , AND EVELYN E. GAISER

Department of Biological Sciences and Southeast Environmental Research Center, Florida International University, Miami, Florida 33199 USA

Citation: Mazzei, V., B. J. Wilson, S. Servais, S. P. Charles, J. S. Kominoski, and E. E. Gaiser. 2020. Periphyton as an indicator of saltwater intrusion into freshwater wetlands: insights from experimental manipulations. *Ecological Applications* 00(00):e02067. 10.1002/eaap.2067

Abstract. Saltwater intrusion has particularly large impacts on karstic wetlands of the Caribbean Basin due to their porous, carbonate bedrock and low elevation. Increases in salinity and phosphorus (P) accompanying saltwater intrusion into these freshwater, P-limited wetlands are expected to alter biogeochemical cycles along with the structure and function of plant and algal communities. Calcareous periphyton is a characteristic feature of karstic wetlands and plays a central role in trophic dynamics, carbon storage, and nutrient cycling. Periphyton is extremely sensitive to water quality and quantity, but the effects of saltwater intrusion on these microbial mats remain to be understood. We conducted an ex situ mesocosm experiment to test the independent and combined effects of elevated salinity and P on the productivity, nutrient content, and diatom composition of calcareous periphyton from the Florida Everglades. We measured periphyton total carbon, nitrogen, and P concentrations and used settlement plates to measure periphyton accumulation rates and diatom species composition. The light and dark bottle method was used to measure periphyton productivity and respiration. We found that exposure to $\sim 1 \text{ g P} \cdot \text{m}^{-2} \cdot \text{yr}^{-1}$ significantly increased periphyton mat total P concentrations, but had no effect on any other response variable. Mats exposed to elevated salinity ($\sim 22 \text{ kg salt} \cdot \text{m}^{-2} \cdot \text{yr}^{-1}$) had significantly lower total carbon and tended to have lower biomass and reduced productivity and respiration rates; however, mats exposed to salinity and P simultaneously had greater gross and net productivity. We found strong diatom species dissimilarity between fresh- and saltwater-treated periphyton, while P additions only elicited compositional changes in periphyton also treated with saltwater. This study contributes to our understanding of how the ecologically important calcareous periphyton mats unique to karstic, freshwater wetlands respond to increased salinity and P caused saltwater intrusion and provides a guide to diatom indicator taxa for these two important environmental drivers.

Key words: *algal mats; diatoms; ecological indicators; phosphorus; salinity; wetlands.*

INTRODUCTION

Karstic, freshwater wetlands located throughout tropical and subtropical coasts in the Caribbean Basin are particularly susceptible to accelerated rates of saltwater intrusion caused by climate change and freshwater diversion. These wetlands are characterized by porous carbonate bedrock and elevations at or near sea level, making them exceptionally vulnerable to saltwater intrusion. Encroachment of saltwater into freshwater marshes alters biogeochemical processes that affect ecosystem carbon and nutrient cycling (Weston et al. 2011, Chambers et al. 2014, Williams et al. 2014, Herbert et al. 2015), causes habitat migration as environmental conditions are modified to favor coastal

communities (Troxler et al. 2014), and eventually leads to coastal transgression, the landward movement of coastlines, with erosion and submergence (Ross et al. 2000, James et al. 2003). The ecological and socioeconomic value of coastal, freshwater wetlands is motivating factors to understand the ecological effects of saltwater intrusion on these vulnerable ecosystems so that appropriate mitigation and restoration activities can be implemented.

Saltwater intrusion is largely driven by rising sea levels, extreme tidal activity, increased storm activity and resultant storm surges, and is exacerbated by reduced freshwater flows to downstream marshes due to freshwater diversion for agricultural and urban purposes (Saha et al. 2011, Briceño et al. 2014, Herbert et al. 2015). The Florida Everglades is a prime example of a karstic, freshwater wetland that is severely threatened by accelerated rates of saltwater intrusion resulting from sea-level rise, particularly in the absence of large-scale

Manuscript received 2 October 2018; revised 11 August 2019; accepted 26 September 2019. Corresponding Editor: Stephen B. Baines.

¹ E-mail: vmazz001@fiu.edu

restoration of freshwater supplies. Historical drainage and channelization of Everglades marshes have lessened freshwater flow into the southern Everglades, leading to reduced groundwater and aquifer recharge in this region (Davis et al. 2005, McCormick et al. 2011, McVoy et al. 2011). The resulting decrease in water table depth allows saltwater intrusion further into the aquifer, increasing groundwater and porewater salinities. A lower water table also allows for overland saltwater intrusion, particularly during storm surges. In addition to elevated salinity, marine water intrusion exposes freshwater marshes to changes in ionic concentration and water chemistry that can alter natural biogeochemical cycles and influence plant and algal productivity. For example, saltwater intrusion increases phosphorus (P) availability in the naturally P-limited Everglades where most P is bound to the limestone bedrock (Williams et al. 2014). The Everglades is described as an “upside down” estuary because, unlike most estuaries, marine water is the dominant source of P to southern Everglades marshes, especially those adjacent to the Gulf of Mexico (Childers et al. 2006). Belowground saltwater intrusion introduces a secondary source of P as saltwater causes CaCO_3 -bound P to be desorbed and made biologically available (Price et al. 2006, Flower et al. 2017). Successful assessments and mitigation strategies of saltwater intrusion into the Everglades requires an understanding of how key ecosystem components, including plants, soil microbes, and periphyton, respond to the simultaneous salinity stress and P subsidies associated with saltwater intrusion.

Calcareous periphyton mats are an important and abundant component of the Florida Everglades and other karstic, freshwater wetlands in the Caribbean Basin (Rejmánková and Komárková 2000, Gaiser et al. 2011, La Hée and Gaiser 2012). In these wetlands, periphyton is characterized by mat-forming microbial assemblages of diatoms, cyanobacteria, chlorophytes, and other microorganisms embedded in a matrix of mucilage and interstitial calcium carbonate secreted by certain resident algal species (Browder et al. 1994, Azim and Asaeda 2005). Periphyton provides a unique microhabitat for a variety of autotrophic and heterotrophic organisms and plays an important role in food web dynamics, water column oxygenation, organic and inorganic carbon cycling, nutrient cycling, and marl soil (calcium carbonate mud) formation (Davis et al. 2005, Hagerthey et al. 2011, Gaiser et al. 2011, Schedlbauer et al. 2012, Troxler et al. 2014, Trexler et al. 2015). Furthermore, periphyton is exceptionally sensitive to water quality changes and responds to these changes with shifts in species composition that, in turn, affect the physical structure and ecological roles of these mats (Browder et al. 1994, McCormick et al. 2001, Gaiser et al. 2006, 2011, Hagerthey et al. 2011).

Changes in both periphyton functional metrics and taxonomic composition provide valuable information about environmental conditions and are often used as bioindicators in ecological assessments of water quality

(P loading) and quantity (hydroperiod) in the Everglades (McCormick and Stevenson 1998, Gaiser et al. 2004, Gaiser 2009). Periphytic diatoms are particularly effective bioindicators given their environmental specificity, quick response times, and species-specific cell wall ornamentation that makes them relatively easy to identify under light microscopy compared with cyanobacteria and chlorophytes (Stevenson et al. 1999, Potapova and Charles 2007, Desrosiers et al. 2013, Stevenson 2014, Taffs et al. 2017). Aside from their indicator value, periphytic diatoms are a numerically dominant component of the periphyton mats, and can contribute to mat cohesion through the production of extracellular mucilage and attachment structures (Johnson et al. 1997, Azim and Asaeda 2005, Gaiser et al. 2010, Lee et al. 2014). Shifts in the composition and relative abundances of diatoms and other mat-engineering species, such as cyanobacteria, are associated with different periphyton mat types, including biofilms and filamentous mats (Vymazal and Richardson 1995, McCormick and O'Dell 1996, Pan et al. 2000, Rejmánková and Komárková 2005, Gaiser et al. 2006). Therefore, diatoms not only provide a useful tool to assess changing salinity and P conditions related to saltwater intrusion, they can also serve as indicators of changes in periphyton mat structure and ecological function caused by increased salinity and P. However, research into the effects of increased salinity and changes in water chemistry, particularly P availability, caused by saltwater intrusion on periphyton and their diatom assemblages is just beginning (Mazzei and Gaiser 2018, Mazzei et al. 2018b). These microbial communities act as first responders to environmental perturbation and can provide managers with advanced notice of impending state changes related to saltwater intrusion that can be used to guide preventative or mitigating measures.

Exposure of aquatic plants and algae to elevated salinity induces physiological stress responses that can be expressed as morphological changes, nutrient-uptake limitations, reduced productivity, and ultimately death (Alam 1999, Mendelsohn and Batzer 2006, Touchette 2007, Affenzeller et al. 2009, Trobajo et al. 2011). These physiological responses by foundation species to salt stress eventually translate to landscape-scale changes in species distributions and ecosystem functions (Ross et al. 2000, James et al. 2003, Troxler et al. 2014). Simultaneous exposure of freshwater periphyton to salt stress and P subsidy, as is expected with saltwater intrusion, may trigger complicated and counterintuitive responses from freshwater, calcareous periphyton. Although nutrient enrichment is generally associated with increased algal growth (Elser et al. 2007) and is expected to ameliorate disturbance stress (Odum et al. 1979), the calcareous periphyton mats of karstic wetlands thrive under P limitation and respond negatively to P loading. The cohesive, calcareous periphyton mats found throughout the short-hydroperiod marshes of the Everglades have been shown to breakdown when exposed to

increased P (McCormick et al. 2001, Gaiser et al. 2006). Although the exact mechanisms behind periphyton breakdown with P enrichment remain poorly understood, there is plenty of evidence demonstrating that P causes changes in mat structure and species composition that result in replacement of native calcareous mats by eutrophic biofilms and filamentous mats that do not provide the same ecological services as calcareous periphyton (Vymazal and Richardson 1995, McCormick and O'Dell 1996, Pan et al. 2000, Rejmánková and Komárová 2005, Gaiser et al. 2006). Therefore, the combination of elevated salinity and P availability caused by saltwater intrusion theoretically represents a two-fold stress on native Everglades periphyton mats.

In this study, we examined the individual and combined effects of elevated salinity and P on the productivity, total carbon, nitrogen, and P content, and diatom composition of calcareous, freshwater periphyton from the Florida Everglades. We proposed three hypotheses: (1) salt exposure reduces periphyton productivity and nutrient uptake and causes shifts in periphytic diatom assemblages from freshwater taxa to euryhaline ones with wider salinity tolerances; (2) addition of P to freshwater periphyton increases mat total P concentrations as P is adsorbed to CaCO_3 particles within the mat and biologically assimilated by the naturally P-limited periphytic communities; P subsidy also increases periphyton productivity but may decrease total carbon content and biomass as species typically associated with calcareous, cohesive periphyton become replaced by filamentous mat- or biofilm-forming eutrophic species; and (3) simultaneous exposure to increased salinity and P will also result in replacement of calcareous, cohesive periphyton by organic mats and biofilms with lower total carbon storage, but potentially more productive than those exposed to elevated salinity alone, and a weedy, euryhaline diatom assemblage.

METHODS

Experimental design

An outdoor mesocosm experiment was conducted at the Florida Bay Interagency Science Center (FBISC) in Key Largo, Florida, USA to test the response of calcareous periphyton mats from oligotrophic, freshwater marshes to elevated salinity and P. Twenty-four sawgrass cores with intact periphyton were collected on July 2014 from an unimpacted freshwater marsh in the Florida Everglades ($25^{\circ}46'06.1''$ N, $80^{\circ}28'56.2''$ W). P load at the harvest site was comparable to or lower than P loading into Everglades National Park and was not considered a nutrient-enriched area (Xue 2018). The cores were transported to FBISC in perforated plastic buckets (0.3 m deep \times 0.4 m wide \times 0.5 m long) lined with mesh. Each perforated plastic bucket holding the cores was placed within a larger, unperforated plastic container (hereafter, "mesocosms," the experimental unit; 0.5 m deep \times 0.5 m

wide \times 0.7 m long). For access purposes, these mesocosms were dispersed across six concrete vaults (0.7 m deep \times 0.8 m wide \times 2.2 m long; Fig. 1A). The four mesocosms within each vault were completely self-contained within the unperforated plastic containers and separated by plastic dividers to avoid any interaction between mesocosms. Each mesocosm was filled with freshwater from the C-111 canal, located near the research facility ($25^{\circ}17'031.74''$ N, $80^{\circ}27'021.59''$ W) and having similar water chemistry to the harvest site, and allowed 8 months to equilibrate before beginning the experiment at the end of March 2015. However, by this time, much of the periphyton collected with the cores had been lost due to transportation and experimental setup, as well as sawgrass overgrowth that caused excessive shading of the periphyton mats. Therefore, before beginning the experiment, we pruned dead leaves from the sawgrass plants and reintroduced fresh periphyton collected from the site where the cores were harvested to each mesocosm (Fig. 1B).

The experimental design consisted of four treatments: freshwater control (F), freshwater with P (FP), saltwater (S), and saltwater with P (SP), with six replicates each (Fig. 1C). The F and FP mesocosms received twice weekly manual additions of freshwater collected from the C-111 canal (~0.2 ppt) to maintain water levels above the soil surface. The S and SP mesocosms were treated with a brine solution consisting of freshwater from the C-111 canal mixed with saltwater from Florida Bay (~32 psu) located adjacent to FBISC. There was no significant difference between canal and Florida Bay water pH, DOC, DIN, NO_3^- , NO_2^- , NH_4^+ , TP, or SRP (Servais et al. 2019, Wilson et al. 2019). Salinity was gradually increased starting in February 2015 until the surface water concentration was within the target range of 5–10 psu (April 2005). The target salinity range was chosen to reflect brackish marsh surface water salinities in the Everglades (Mazzei et al. 2018). Salinity was maintained within this range by manually adding brine twice weekly. The concentration of the brine was adjusted as needed based on the salinities of the mesocosms on the day of dosing to maintain salinity within the target. The FP and SP mesocosms received continuous delivery of 2.25 mg/L diluted phosphoric acid (H_3PO_4) at 0.14 mL/minute via two multichannel peristaltic pumps with six lines each (Watson Marlow; Wilmington, Massachusetts, USA) to achieve a target P loading rate of $\sim 1 \text{ g P} \cdot \text{m}^{-2} \cdot \text{yr}^{-1}$. This loading rate is similar to the assimilative capacity reported for periphyton by Gaiser et al. (2005), and all levels of above-ambient exposure to P have been found to stimulate a response from periphyton (McCormick and O'Dell 1996, McCormick and Stevenson 1998, McCormick et al. 2001).

Abiotic measurements

Cumulative salinity loads in each mesocosm were measured as the added molar mass of chloride based on weekly salinity measures and the total volume of elevated source water added to each salinity treatment

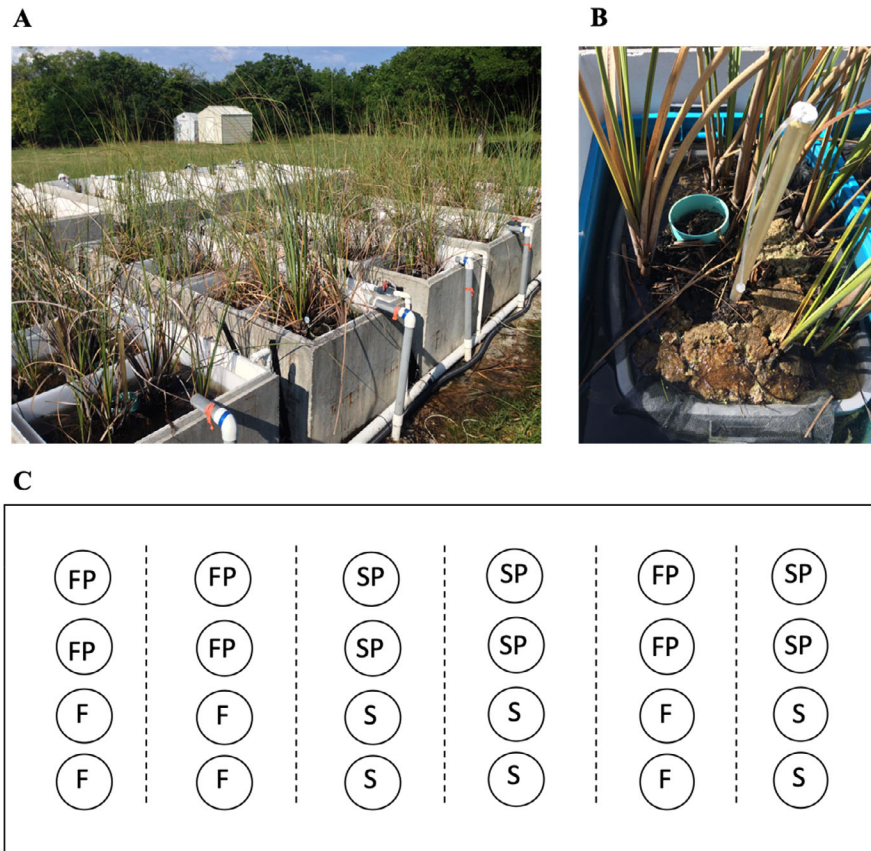


FIG. 1. Layout of the 24 mesocosms. (A) Mesocosms were completely self-contained with no interaction between adjacent mesocosms; the concrete tubs were not part of the treatments but served to drain overflow from dosing the mesocosms and keep the surrounding area clean. (B) Close-up of an individual mesocosm. (C) Conceptual diagram of the experimental design; mesocosms were arranged as shown to avoid or reduce error associated with accidental cross-contamination when administering treatments and collecting samples. Circles represent mesocosms and letters designate the treatment each core received (F, freshwater control; FP, freshwater and phosphorus; S, salinity; SP, salinity and phosphorus).

mesocosm. Cumulative phosphorus loads were measured for each mesocosm as the daily added molar mass of P delivered to P treatment mesocosms plus the added molar mass of P from freshwater and elevated salinity source waters (based on monthly measures and the total volume of source water added to each mesocosm).

Surface and porewater temperature, pH, and salinity in each mesocosm were measured twice a week during the fresh and saltwater additions using a YSI Model 600 XL (Xylem, Yellow Springs, Ohio, USA). Porewater samples were obtained from porewater sippers with an air stone (4 cm long \times 1 cm diameter) installed within each mesocosm at 15 cm depth at the start of the experiment. Total P (TP), total nitrogen (TN), and total organic carbon (TOC) in unfiltered surface water samples were measured monthly at the Southeast Environmental Research Center Nutrient Analysis Laboratory at Florida International University. Filtered surface and porewater samples were also analyzed monthly for soluble reactive P (SRP), dissolved inorganic nitrogen (DIN; NO_3^- , NO_2^- , NH_4^+), and dissolved organic carbon

(DOC). Complete water chemistries are beyond the scope of this manuscript (see Servais et al. 2019, Wilson et al. 2019)

Periphyton mats

Periphyton mat subsamples of 10 mL were collected bimonthly, starting in April 2015, from each mesocosm using a plastic syringe. In the lab, the mat samples were placed in a 500-mL beaker and homogenized with deionized water (DI) water to a periphyton slurry with a minimum volume of 200 mL. The beaker was placed on a stir plate to facilitate continuous mixing while the slurry was subsampled for biomass, chl *a*, total carbon (TC), total nitrogen (TN), and total phosphorus (TP) analyses. The biomass and chl *a* subsamples were analyzed using the same methods described for the settlement plate samples. The TP subsample was dried at 80°C and pulverized with a mortar and pestle. We processed a known amount of each subsample and used colorimetric analyses to estimate TP concentration, expressed as $\mu\text{g P/g}$.

AFDM, following the methods of Solórzano and Sharp (1980). TC and TN subsamples were ground down to a fine powder by mortar and pestle, dried at 60°C, and analyzed for total C and N content using a Flash 1112 elemental analyzer (CE Elantech, Lakewood, New Jersey, USA) following standard procedures.

Periphyton metabolism was measured on February 2016 using the light and dark bottle technique to measure biological oxygen demand (BOD). Two 10-mL periphyton samples were collected from each mesocosm; one was placed in a 300-mL clear bottle to measure periphyton net ecosystem productivity (NEP), and the other was placed in a 300-mL dark bottle to measure periphyton ecosystem respiration (ER). NEP and ER were also measured in a blank light and blank dark bottle filled only with source water. The paired clear and dark BOD bottles were filled with source water and initial dissolved oxygen (DO) concentrations were measured using a YSI ProODO Dissolved Oxygen Meter (YSI, Yellow Springs, Ohio, USA). The bottles were topped off with source water before capping the bottles to avoid air bubbles. The bottles were then submerged in an outdoor water bath, where they incubated for 2 h under ambient light and temperature. After the incubation period, final DO concentrations were measured and the periphyton from the light bottles was transported back to the lab for further analyses as previously described. The change in DO measured in the blank light and dark bottles was subtracted from all other light and dark bottles to account for productivity and respiration in the water column (i.e., non-periphyton metabolism). NEP and ER were standardized to the ash-free dry mass (AFDM) of the incubated sample and the measured oxygen production and consumption rates were converted to $\text{mg C}\cdot\text{g AFDM}^{-1}\cdot\text{h}^{-1}$ by multiplying NEP and ER by the mass ratio of C:O₂ (0.357) and then dividing NEP by a photosynthetic quotient of 1.2 and ER by a respiratory quotient of 1. Gross primary productivity (GPP) was then calculated by adding the absolute value of the ER value to NEP.

Periphyton settlement plate measurements

We deployed clear, acrylic settlement plates ($\sim 104 \text{ cm}^2$) in each mesocosm to measure periphyton biomass and chlorophyll *a* accumulation rates and to analyze diatom species composition. The settlement plates were incubated on the soil surface of the mesocosm for two months to allow periphyton mats in the mesocosms to colonize the plates. At the end of the two-month incubation period, settlement plates were retrieved and transported to the laboratory, where they were scraped clean using a razor blade and deionized water. Settlement plates were sterilized using a bleach solution and redeployed the following month. This was done quarterly from March 2015 to April 2016 for a total of four settlement plate samples per mesocosm over the duration of the experiment.

The material scraped from the settlement plates was collected in a beaker and homogenized with deionized water (DI) water to a minimum volume of 200 mL. The beaker was placed on a stir plate to facilitate continuous mixing while the slurry was subsampled for biomass, chlorophyll *a*, and diatom analysis. The biomass subsample was placed in a drying oven at 80°C for ≥ 48 h to obtain a dry mass (g) measurement and then in a furnace where it was combusted at 500°C for 1 h to obtain the ash (mineral) mass (g). We calculated ash-free dry mass (AFDM) by the loss-on-ignition method as the difference between the ash mass and the total dry mass. The chl *a* subsample was filtered onto Whatman 25-mm diameter glass fiber filter (GFF) paper, frozen, and later subjected to 48 h 90% cold acetone extraction at 20°C. Chl *a* concentrations were determined using a Gildford FLUORO IV fluorometer (Gildford Instrument, Oberlin, Ohio, USA; excitation 435 nm; emission 667 nm). AFDM and chl *a* accumulation rates ($\text{mg}\cdot\text{m}^{-2}\cdot\text{d}^{-1}$) were calculated by standardizing AFDM and chl *a* values by the area of the settlement plates and the number of days incubated.

Diatom subsamples were cleaned of mineral debris and organic matter using the sulfuric acid oxidation methods prescribed by Hasle and Fryxell (1970). We pipetted a known volume of cleaned diatom sample onto a glass coverslip, permanently mounted it on a microscope slide with Naphrax (PhycoTech, St. Joseph, Michigan, USA) mounting medium, and viewed the diatoms under a compound light microscope (Axioskop 2; Zeiss, Thornwood, New York, USA) equipped with differential interference contrast and a digital camera (Leica DFC425, Wetzlar, Germany). We counted at least 500 diatom valves along random transects at 600 \times magnification under oil immersion and identified them to the species level. Raw diatom counts were converted to relative abundance by standardizing the number of valves counted for each species by the total number of valves counted. We chose to analyze periphyton diatom species composition from the settlement plates rather than samples taken from the mesocosm soil surface because, as diatoms are counted and identified from cleaned (oxidized) samples, testing treatment effects on the diatom assemblage using established mats would have been confounded by the presence of dead diatom frustules; using settlement plates allowed us to better pick up diatom community response to treatments over time.

Statistical analyses

We used univariate analysis of variance (ANOVA) and Tukey's post hoc test to determine if salinity, total salt load, and salt loading rate were significantly higher in S and SP treatments compared with the F and FP treatments, and if surface water TDP, total P load, and P loading rate were greater in FP and SP compared with F and S treatments.

Three separate one-way multivariate ANOVAs (factor = treatment, levels = F, FP, S, SP) were used to

assess differences in periphyton functional responses across treatments (IBM SPSS Statistics V23.0, IBM, Armonk, New York, USA). A one-way MANOVA was used to statistically compare periphyton TC, TN, TP, and chl *a* concentrations across the four treatments. A second one-way MANOVA was used to test for treatment effects on AFDM and chl *a* accumulation rates on the settlement plates. A third one-way MANOVA was used to test for differences in periphyton NEP, ER, and GPP among treatments. All MANOVAs were followed with Tukey's post hoc pairwise comparisons to look for significant differences among treatments.

Diatom compositional dissimilarity (settlement plates) among treatments was analyzed by analysis of similarity (ANOSIM). Nonmetric multidimensional scaling (NMDS) was used to visualize Bray-Curtis dissimilarity among treatment groups (PRIMER v6, Albany, New Zealand, Clarke and Gorley 2006). Indicator species for each treatment group and combinations of treatment groups were determined using the multi-level pattern analysis function available in the indicspecies package (multipatt {indicspecies}) (De Cáceres et al. 2010, De Cáceres 2013) in the R statistical environment (R Core Team, v. 3.3.3, 2017).

RESULTS

Saltwater and phosphoric acid additions

The addition of saltwater significantly elevated mean surface water salinity in the S (8.4 ± 4.1 psu, $n = 96$) and SP (8.2 ± 3.9 psu, $n = 96$) treatments compared

with the F (0.5 ± 0.3 psu, $n = 96$) and FP (0.4 ± 0.2 psu, $n = 96$) treatments across all sampling dates and on all individual sampling dates (Table 1, Fig. 2, Lee et al. 2019). Total cumulative salt added to the S treatments by the end of the experiment (July 30th, 2016) was $\sim 22 \times$ the salt load in F treatments. There was no difference in salinity between the S and SP treatments (Tukey $P = 0.967$) nor between the F and FP treatments (Tukey $P = 0.999$). Salinity in the two freshwater treatments remained steady throughout the experiment, whereas salinity in the S and SP treatments fluctuated over time and experienced higher than average concentrations during summer months (May – Aug 2015) likely resulting from accumulation of salts from evaporative loss.

FP and SP treatments received ~ 1 g P·m $^{-2} \cdot$ yr $^{-1}$ (accounting for both the phosphoric acid drip and P concentrations in the source waters) and a total cumulative P load $\sim 54 \times$ greater than in F and S treatments by the end of the experiment (Table 1, Fig. 2). Although mean surface water TDP was nearly doubled in FP (35.6 ± 21.7 $\mu\text{g/L}$, $n = 96$) compared with F (16.5 ± 14.2 $\mu\text{g/L}$, $n = 96$) treatments, this difference was not statistically significant (Tukey $P = 0.854$, Table 1). Mean TDP in S treatment plots (45.6 ± 101.8 $\mu\text{g/L}$, $n = 96$) was not significantly different than either F (Tukey $P = 0.616$) or FP (Tukey $P = 0.976$). The SP treatment had the highest mean TDP concentrations (172.0 ± 316.1 $\mu\text{g/L}$, $n = 96$) and was significantly different from all three other treatments (Tukey $P < 0.001$). TP in the fresh (5.2 ± 4.2 $\mu\text{g/L}$) and saltwater (7.6 ± 4.7 $\mu\text{g/L}$) sources (C-111 canal and Florida Bay,

TABLE 1. Means and standard deviations (SD) of total cumulative salt added through 30 July 2016, salt loading rate, surface water (SW) salinity (SAL), total cumulative P added through 30 July 2016, P loading rate, and total dissolved phosphorus (TDP); chlorophyll *a* (chl *a*), total carbon (TC), total nitrogen (TN), and total phosphorus (TP) content of periphyton; and ash-free dry mass (AFDM) and chl *a* accumulation rates on settlement plates averaged over all sampling dates for each treatment.

Measure	F		FP		S		SP	
	Mean	SD	Mean	SD	Mean	SD	Mean	SD
Abiotic								
Total salt load (kg/m 2)	0.2 ^a	0.0	0.3 ^a	0.1	5.2 ^b	0.2	5.0 ^b	0.3
Salt loading rate (kg·m $^{-2} \cdot$ yr $^{-1}$)	0.9 ^a	0.2	1.1 ^a	0.5	22.5	1.1	21.6	1.4
SW SAL (ppt)	0.5 ^a	0.3	0.4 ^a	0.2	8.4 ^b	4.1	8.2 ^b	3.9
Total P load (g/m 2)	0.0 ^a	0.0	0.3 ^b	0.0	0.0 ^a	0.0	0.3 ^b	0.0
P loading rate (g·m $^{-2} \cdot$ yr $^{-1}$)	0.0 ^a	0.0	1.0 ^b	0.0	0.0 ^a	0.0	1.0 ^b	0.0
SW TDP ($\mu\text{g/L}$)	16.5 ^a	14.2	35.6 ^a	21.7	45.6 ^a	101.8	172.0 ^b	316.1
Periphyton mats								
Chl <i>a</i> (mg/g AFDM)	2.3 ^a	4.7	3.2 ^a	2.2	1.7 ^a	1.3	3.0 ^a	2.1
TC (mg/g)	282.6 ^a	69.1	278.6 ^a	33.0	233.9 ^b	34.9	233.3 ^b	47.0
TN (mg/g)	14.3 ^{ab}	6.2	17.7 ^a	5.7	12.6 ^b	3.8	15.5 ^{ab}	7.6
TP ($\mu\text{g/g}$)	264.6 ^a	160.9	516.2 ^b	208.6	206.3 ^a	111.1	664.3 ^b	497.3
Settlement plates								
AFDM (mg·m $^{-2} \cdot$ d $^{-1}$)	88.3 ^a	84.3	86.7 ^a	81.1	70.8 ^a	71.0	58.8 ^a	47.0
Chl <i>a</i> ($\mu\text{g} \cdot \text{g AFDM}^{-1} \cdot \text{d}^{-1}$)	114.9 ^a	60.4	161.7 ^a	73.8	120.1	81.0	134.4 ^a	87.1

Notes: Different superscript letters indicate significant differences ($P < 0.05$) among treatments. Treatments are F, freshwater; FP, freshwater and phosphorus; S, saltwater; SP, saltwater and phosphorus.

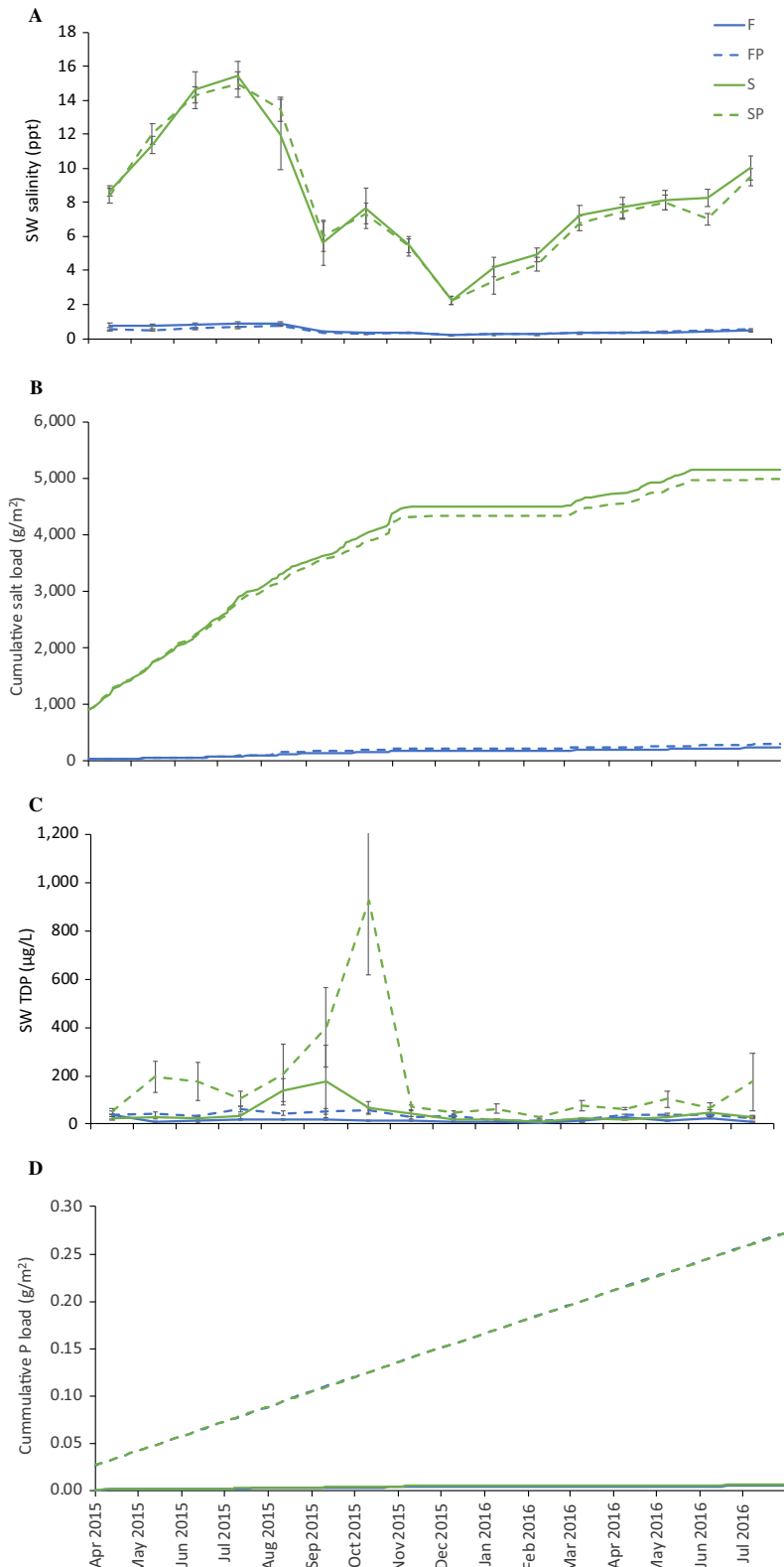


FIG. 2. Monthly surface water (SW) (A) salinity, (B) cumulative salt load, (C) SW total dissolved phosphorus (TDP), and (D) cumulative phosphorus (P) load across treatments ($n = 6$). Error bars show standard error. F, freshwater control; FP, freshwater and phosphorus; S, salinity; SP, salinity and phosphorus.

respectively) was not significantly different ($t_7 = -0.97$, $P = 0.36$).

Functional and chemical responses to salinity and P

The TP, TN, and chl-*a* content of periphyton mats averaged over the length of the experiment tended to be higher in P treatments, regardless of salt treatment, although these trends were not always statistically significant (Table 1, Fig. 3). Periphyton TP was significantly higher in the FP ($516.2 \pm 208.6 \mu\text{g/g}$, $n = 32$) and SP ($664.3 \pm 497.3 \mu\text{g/g}$, $n = 33$) treatments relative to F ($264.6 \pm 160.9 \mu\text{g/g}$, $n = 33$) and S ($206.3 \pm 111.1 \mu\text{g/g}$, $n = 37$) treatments (Tukey $P < 0.01$) and was not significantly different between F and S (Tukey $P = 0.826$) nor between FP and SP (Tukey $P = 0.157$) treatments. Periphyton TN tended to be higher in mesocosms treated with P relative to those without added P, particularly in 2016, but this effect was not statistically significant when averaged over all dates (Tukey $P > 0.1$). Periphyton TC concentration was unaffected by the P treatments but was significantly lower in salinity compared with freshwater treatments (Tukey $P < 0.001$). We found no significant treatment effects on chl-*a* concentrations (Tukey $P > 0.05$), but we did observe a strong trend of elevated chl-*a* in P-treated mats and decreased periphyton chl-*a* concentrations in S compared with F treatments. The effects sizes, reported here as partial eta squared, for the four dependent variables, TP, TN, TC, and chl-*a*, in this MANOVA model were 0.31, 0.09, 0.20, and 0.04 respectively.

Accumulation rates of periphyton AFDM and chl-*a* measured from settlement plate samples were not different ($P > 0.05$) across treatments, but showed general trends like those seen for TC and chl-*a* concentrations in periphyton mats (Table 1, Fig. 4). AFDM accumulation rates tended to be lower in S than in F treatments and were the lowest in SP treatments. A general pattern of decreasing AFDM accumulation rates over time was also observed. A trend towards greater, biomass-specific chl-*a* accumulation rates in P-treated periphyton was observed for both F and S mats. The effect size for AFDM accumulation rate was 0.3 and 0.6 for chl-*a* accumulation rate.

Mean periphyton NEP and GPP were lower in the S (1.6 ± 0.8 and $3.1 \pm 1.3 \text{ mg C}\cdot\text{g AFDM}^{-1}\cdot\text{h}^{-1}$, respectively, $n = 5$) than the F (2.5 ± 2.0 and $7.2 \pm 6.2 \text{ mg C}\cdot\text{g AFDM}^{-1}\cdot\text{h}^{-1}$, respectively, $n = 3$) and FP (2.8 ± 2.2 and $5.7 \pm 2.1 \text{ mg C}\cdot\text{g AFDM}^{-1}\cdot\text{h}^{-1}$, respectively) treatments, but these differences were not statistically significant (Tukey $P > 0.05$, Fig. 5). No significant difference in periphyton NEP was detected between F and FP treatments ($P > 0.05$). Likewise, there was no statistical difference in periphyton GPP between F and FP treatments (Tukey $P > 0.05$). However, in salt-treated periphyton, the addition of P significantly increased NEP ($9.6 \pm 2.8 \text{ mg C}\cdot\text{g AFDM}^{-1}\cdot\text{h}^{-1}$, $n = 3$, Tukey $P = 0.001$) and GPP ($12.2 \pm 3.1 \text{ mg C}\cdot\text{g AFDM}^{-1}\cdot\text{h}^{-1}$,

$n = 3$, Tukey $P = 0.018$) compared with mats treated with elevated salinity alone. Periphyton ER was not affected by any of the treatments (Tukey $P > 0.05$), although mean ER was lowest in S treatments ($-1.5 \pm 0.7 \text{ mg C}\cdot\text{g AFDM}^{-1}\cdot\text{h}^{-1}$, $n = 5$). The effect size for NEP, GPP, and ER was 0.79, 0.59, 0.31, respectively.

The relationship between increasing P loads and periphyton TP, TC, TN, chl-*a*, AFDM accumulation rates, chl-*a* accumulation rates, and surface water TDP across treatments is shown in Appendix S1: Fig. S1.

Diatom assemblage responses to salinity and phosphorus

The diatom assemblages of periphyton mats subjected to the F and S treatments formed two distinct groups in the NMDS ordination; the ANOSIM confirmed these groups were significantly dissimilar (Table 2, Fig. 5). Surprisingly, the addition of P to freshwater periphyton (FP) did not cause significant taxonomic divergence from freshwater control (F) mats. However, both F and FP were significantly different from S and SP. The greatest divergence in taxonomic composition occurred between FP and SP treatments and between F and SP. The SP treatment resulted in a significantly different diatom assemblage than that of S treatments.

The multi-level pattern analysis identified 18 significant indicators out of a total of 56 taxa (Table 3). The three freshwater indicators (F treatment) were species typically associated with oligotrophic, calcareous periphyton in the Everglades. Although, the ANOSIM showed that the diatom assemblages of the F and FP treatment were not significantly different, the indicator species analysis classified three species of *Gomphonema*, two species of *Nitzschia*, and *Kobayasiella subtilissima*, as indicator taxa of enriched, freshwater conditions (FP treatment). The analysis also identified four indicators of the S treatment, two *Fragilaria* and two *Mastogloia* species; these species were nearly absent in the two freshwater treatments. Indicator species of the SP treatment, including two *Amphora* species, *Mastogloia braunii*, *Navicula salinicola*, and *Rhopalodia pacifica*, were also absent from both freshwater treatments and significantly lower in the S only treatment (Figs. 6, 7).

DISCUSSION

Accelerated rates of saltwater intrusion threaten coastal, freshwater wetlands globally. Sea-level rise and declines in freshwater inflows with increasing human demands have intensified saltwater intrusion and altered natural salinity and P gradients in the Florida Everglades. Our results indicate that exposure to elevated salinity affects the functioning and diatom community composition of freshwater, calcareous periphyton more strongly than P, resulting in lower productivity, TC concentration, and a distinct salt-tolerant diatom assemblage. However, while the addition of P to freshwater

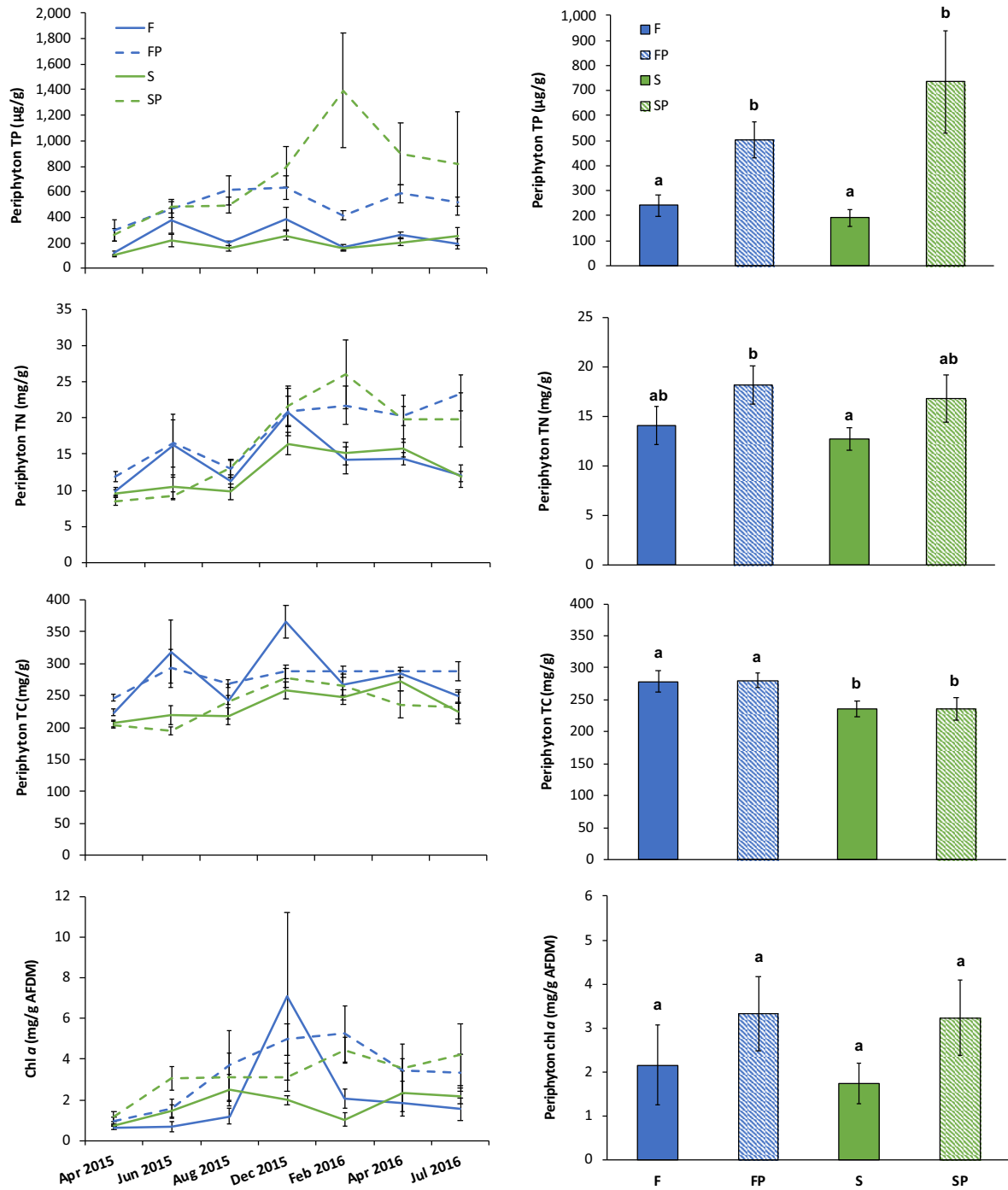


Fig. 3. Bimonthly mean periphyton total phosphorus (TP), total nitrogen (TN), total carbon (TC), and chlorophyll *a* (chl *a*) across treatments ($n = 6$) (left) and overall response means for each treatment averaged over the length of the experiment (right). AFDM, ash-free dry mass. Error bars show standard error. Different lowercase letters indicate significant differences ($P < 0.05$) among treatments. F, freshwater control; FP, freshwater and phosphorus; S, salinity; SP, salinity and phosphorus.

mats did little other than raise mat TP concentrations, the addition of P to salt-treated mats raised mat TP, productivity, chl-*a*, and caused a shift in the diatom assemblage to eutrophic, salt-tolerant assemblage.

Despite SP-treated mats exhibiting the highest productivity, their TC concentrations were as low as mats from the S treatment suggesting that elevated salinity, regardless of P availability, causes the replacement of

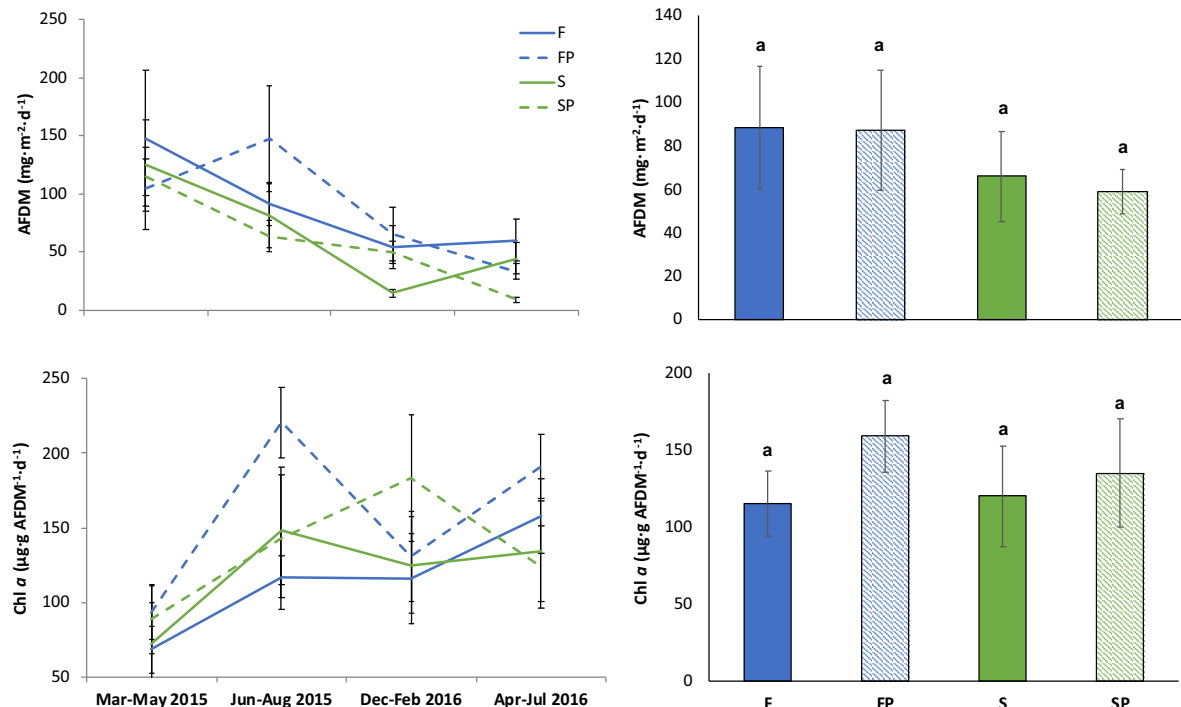


FIG. 4. Periphyton ash-free dry mass (AFDM) and chlorophyll *a* (chl *a*) accumulation rates measured quarterly from settlement plates. Error bars show standard error. Different lowercase letters indicate significant differences ($P < 0.05$) among treatments. F, freshwater control; FP, freshwater and phosphorus; S, salinity; SP, salinity and phosphorus.

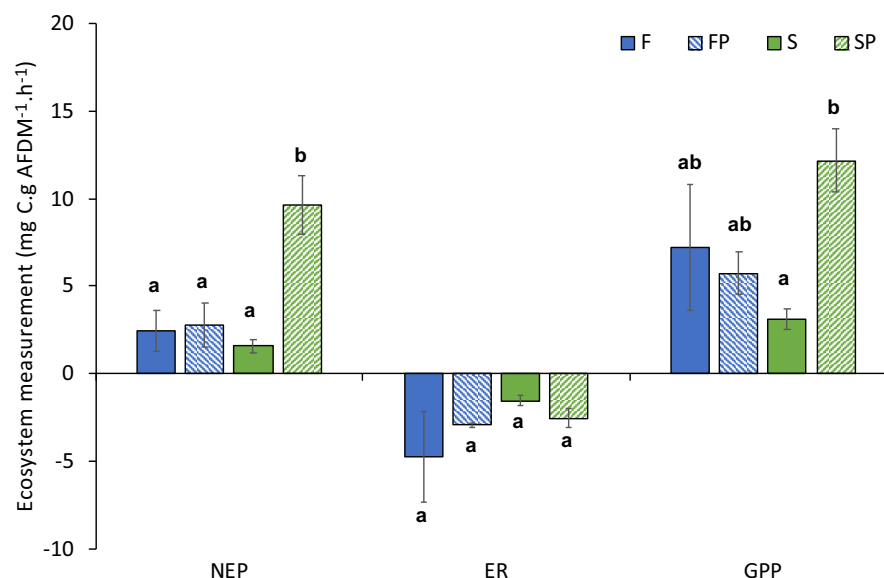


FIG. 5. Periphyton net ecosystem productivity (NEP), ecosystem respiration (ER), and gross primary productivity (GPP) one-time measurements on periphyton plugs collected on February 2016. Error bars indicate standard error. Different lowercase letters indicate significant differences ($P \leq 0.05$) among treatments for each variable based on MANOVA post hoc pair-wise comparisons across treatment groups. F, freshwater control; FP, freshwater and phosphorus; S, salinity; SP, salinity and phosphorus.

TABLE 2. Analysis of similarity (ANOSIM) pair-wise comparisons of recruitment communities from settlement plates among the four treatments. Asterisks show significant P-values at $\alpha = 0.05$

Treatment	F		FP		S		F + FP (all fresh)		F + S (all no P)	
	R	P	R	P	R	P	R	P	R	P
FP	0.091	0.09								
S	0.576	0.001*	0.667	0.001*						
SP	0.689	0.001*	0.663	0.001*	0.393	0.001*				
S + SP (all + salt)							0.554	0.001		
FP + SP (all + P)									0.126	0.005

Notes: Results of ANOSIM comparing recruitment community composition between all freshwater (F + FP) and all saltwater (S + SP) treatments and between all no P (F + S) and all + P (FP + SP) treatments are also reported.

TABLE 3. Indicator taxa for each treatment group determined from indic species analysis ($P < 0.05$) with mean relative abundances for each indicator species in each of the four treatment groups treatments.

Treatment group and taxon number	Taxon	Authority	F	FP	S	SP
F						
1	<i>Achnanthes minutissima</i>	Kützing, 1833	0.014	0.007	0.003	0.001
2	<i>Brachysira microcephala</i>	(Grunow) Compère, 1986	0.250	0.051	0.053	0.013
3	<i>Encyonopsis microcephala</i>	(Grunow) Krammer, 1997	0.081	0.014	0.002	0.001
FP						
4	<i>Gomphonema clavatum</i>	E. Reichardt, 1999	0.000	0.033	0.000	0.000
5	<i>Gomphonema intricatum vibrio</i>	(Ehrenberg) Cleve, 1894	0.094	0.173	0.002	0.006
6	<i>Gomphonema parvulum</i>	Kützing, 1849	0.009	0.104	0.000	0.001
7	<i>Kobayasiella subtilissima</i>	Lange-Bertalot, 1999	0.006	0.014	0.000	0.000
8	<i>Nitzschia amphibia</i>	Grunow, 1862	0.188	0.245	0.025	0.031
9	<i>Nitzschia ftsp16</i>		0.001	0.025	0.000	0.000
S						
10	<i>Fragilaria ftsp16</i>		0.000	0.003	0.241	0.016
11	<i>Fragilaria minuscula</i>	(Grunow) Williams, 1987	0.000	0.000	0.012	0.002
12	<i>Mastogloia vmsp01</i>		0.000	0.000	0.004	0.000
13	<i>Mastogloia lanceolata</i>	Thwaites ex W. Smith 1856	0.000	0.000	0.130	0.031
SP						
14	<i>Amphora coffeaeformis aponina</i>	Archibald & Schoeman, 1984	0.001	0.000	0.076	0.346
15	<i>Amphora punctata</i>	Stepanek and Kociolek, 2013	0.000	0.000	0.029	0.097
16	<i>Mastogloia braunii</i>	Grunow, 1863	0.000	0.001	0.000	0.016
17	<i>Navicula salinicola</i>	Hustedt, 1939	0.000	0.000	0.015	0.060
18	<i>Rhopalodia pacifica</i>	Lange-Bertalot & Krammer, 1987	0.000	0.000	0.000	0.036

calcareous mats having high inorganic C content by non-calcareous mats.

Functional and chemical responses to salinity and phosphorus

Osmotic stress and ionic toxicity associated with exposure to elevated salinity can decrease chlorophyll content, photosynthetic electron transport activities, and the uptake of essential nutrients in non-salt-adapted autotrophs (Lu and Vonshak 2002, Sudhir and Murthy 2004, Hu and Schmidhalter 2005). Mazzei et al. (2018) reported reduced productivity, TC, TN, and TP content uptake in freshwater periphyton mats from the Everglades exposed to experimentally elevated salinity in a

field mesocosm study. Here, we found similar effects of elevated salinity on periphyton productivity expressed as lower NEP, GPP, chl-a, TC content, and AFDM accumulation rates in salt-treated compared with freshwater mats. However, we did not see significant reductions in TN and TP in salt-exposed compared with freshwater mats. This can be explained by the complete shift in diatom, and presumably other algal species, composition from a freshwater to salt-tolerant assemblage with continuous exposure to higher salinities (Florida Bay source water inoculum) whose nutrient-uptake ability was unaffected by salt stress. Because nitrite, nitrate, ammonium, TP, and SRP concentrations in fresh and salt source waters were not significantly different, our S treatment did not provide N or P subsidies (Servais et al. 2019,

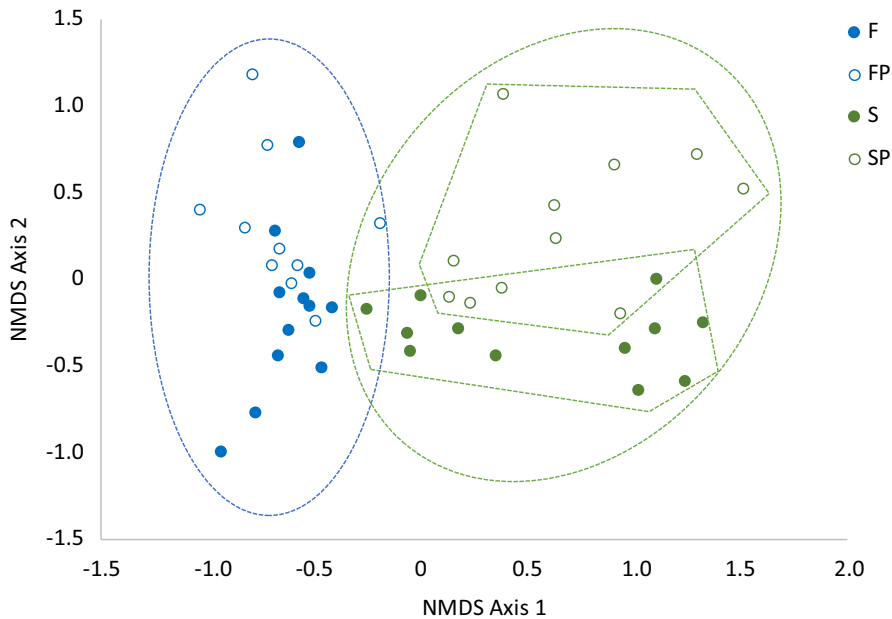


FIG. 6. Nonmetric multidimensional scaling ordination of diatom species dissimilarity, determined from settlement plates, among treatments (F, freshwater; FP, freshwater and phosphorus; S, saltwater; SP, saltwater and phosphorus) across the four sampling dates. Convex hulls are drawn around significantly dissimilar groupings (see Table 2).

Wilson et al. 2019). Declines in periphyton productivity with experimentally elevated salinity have also been reported from karstic wetlands in Belize (Rejmánková and Komárková), however, the effects of salinity on periphyton ER were not reported in that publication. Based on evidence that elevated salinity increases soil microbial respiration in wetlands (Weston et al. 2011, Chambers et al. 2014) periphyton could be expected to respond similarly because these mats host bacterial as well as algal communities. This assumption was not supported by the current study, where ER rates, were lower, albeit not significantly, in S compared with F treatments. Likewise, the only other study to test the effect of elevated salinity on periphyton productivity in the Everglades found non-significant declines in periphyton ER in salt-exposed mats (Mazzei et al. 2018). These results suggest that elevated salinity results in metabolic stress that reduces overall productivity and respiration in the periphyton micro-ecosystem. Testing the effects of elevated salinity on algal and bacterial components of periphyton separately is an important next step in understanding the mechanisms of overall reduction in periphyton metabolic activity.

As expected, P-treated periphyton exhibited significantly higher TP concentrations than mats that did not receive a P treatment regardless of the salinity treatment. Periphyton rapidly assimilates and stores P through both biotic and abiotic pathways, effectively removing excess P from the environment (Scinto and Reddy 2003). This rapid uptake of P by periphyton likely explains why we did not detect significantly greater surface water TDP

concentrations in F compared with FP treatments. Release from nutrient limitation usually results in increased productivity but, despite higher TP concentrations in FP-treated mats, we did not detect elevated NEP or GPP in these mats compared with those from the F treatment. Biomass-specific chl-*a* concentrations in periphyton mats and biomass-specific chl-*a* accumulation rates on settlement plates were also not significantly different between F and FP treatments, although they tended to be higher in the FP treatment. These results suggest that most of the P taken up by the mats in the FP treatment was through the abiotic pathway of adsorption to CaCO₃ in the mats so that it was not biologically available for algal growth. On the other hand, addition of P to salt-treated mats significantly increased NEP and GPP compared with mats from any other treatment and increased chl-*a* concentrations in SP compared with S treatments. Saltwater has been shown to cause P desorption from CaCO₃ bedrock in the Everglades (Price et al. 2006, Flower et al. 2017), and a similar mechanism may be at play within the calcareous periphyton mats. Unlike the FP treatments, where added P was likely bound to CaCO₃ particles in calcareous periphyton, P taken up by mats exposed to the SP treatment maybe more biologically available as anion competition makes it harder for P to bind to CaCO₃ in the mats. This would explain the increased productivity observed in periphyton subjected to elevated salinity and P simultaneously and suggests that P availability potentially mitigates salt stress. However, despite greater productivity in SP-treated mats, the significantly lower TC

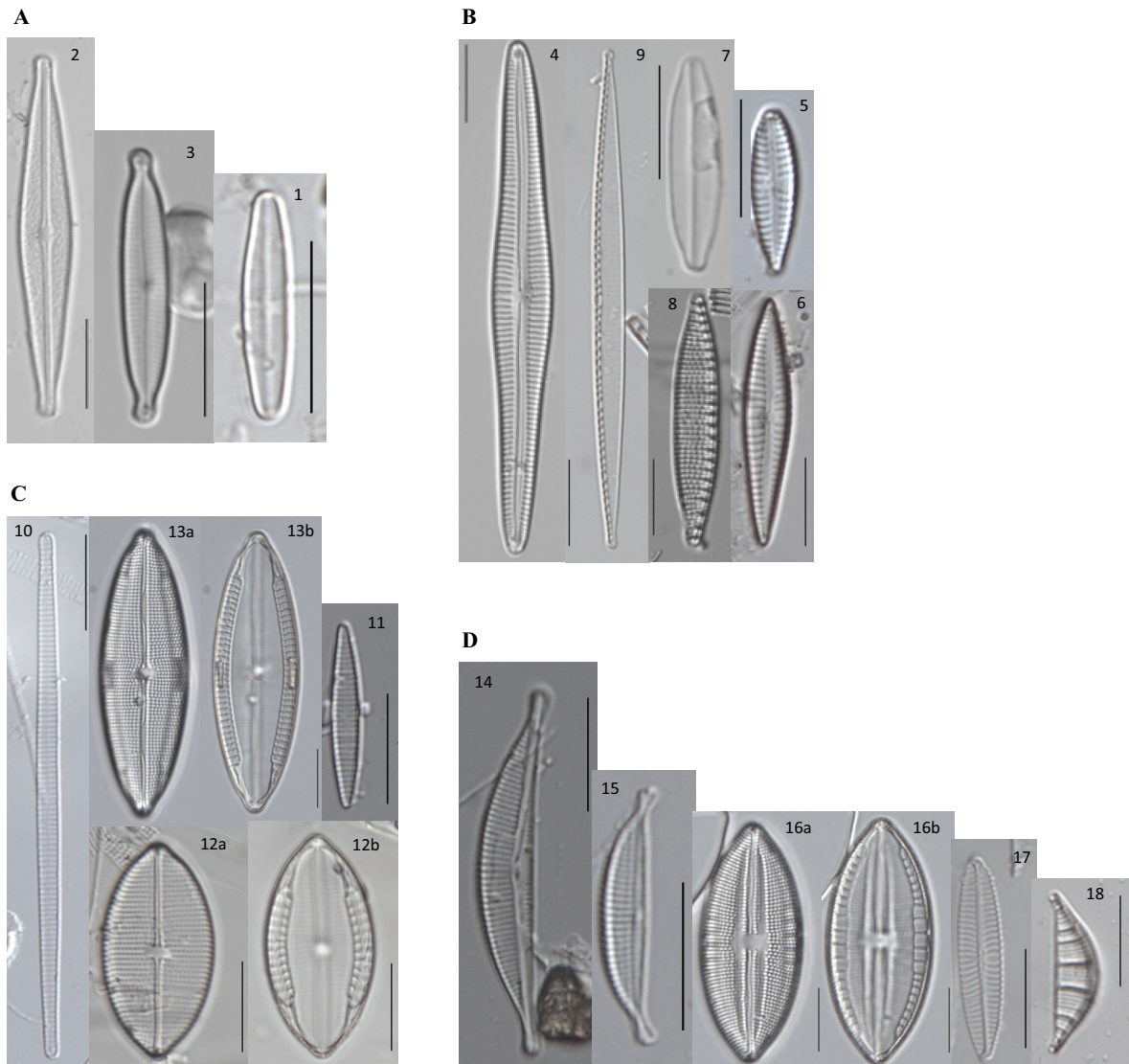


FIG. 7. Indicator taxa plates for (A) freshwater, (B) freshwater and phosphorus, (C) salinity, and (D) salinity and phosphorus treatments. Number corresponds to species number in Table 3. Scale bars = 10 μ m.

content in salt-treated mats suggests that cohesive, calcareous mats, with high inorganic C content, are lost with exposure to elevated salinity and replaced by highly productive, non-calcareous mats or biofilms that may not provide the same ecosystem functions as native calcareous periphyton.

Surprisingly, we did not see significant reductions in periphyton TC or AFDM accumulation rates with added P despite evidence that calcareous periphyton mats breakdown with continuous, low-level P inputs (Gaiser et al. 2005, 2006). It is possible that the P loading rate in this experiment (~ 1 g P·m $^{-2} \cdot$ yr $^{-1}$) was not high enough to illicit a structural response resulting in mat breakdown given that our loading rate was equal to the P assimilative capacity, the quantity of P that can be

assimilated without any significant ecosystem change, reported by Richardson and Qian (1999) for North American wetlands. However, assimilation rates are parameter dependent; Gaiser et al. (2005) report an assimilative capacity for periphyton mat TP concentration near 0 g P·m $^{-2} \cdot$ d $^{-1}$ but an assimilative capacity of 0.1 g P·m $^{-2} \cdot$ d $^{-1}$ for periphyton cover and 1.5 g P·m $^{-2} \cdot$ d $^{-1}$ for periphyton diatom composition from a flume experiment conducted in a pristine marsh in the Everglades. These findings complement our results showing that periphyton TP concentrations rapidly respond to low-level P inputs while changes in periphyton biomass and diatom composition require higher level P inputs. Another study by McCormick et al. (2001) used a field mesocosm experiment to test

periphyton response to P enrichment in an oligotrophic marsh and found that calcareous periphyton began to breakdown and become replaced by eutrophic organic mats at $1.6\text{--}3.2\text{ g P}\cdot\text{m}^{-2}\cdot\text{yr}^{-1}$, higher than our loading rate.

The exact mechanisms behind calcareous mats breakdown with P enrichment are uncertain. One possible mechanism of calcareous periphyton breakdown is the loss of the calcium carbonate precipitating, cyanobacterial species *Schizothrix* and *Scytonema* as they are outcompeted by eutrophic species. A second possibility is potentially higher bacterial respiration rates within the mats. Because periphyton absorb and store P quickly, P enrichment may increase bacterial respiration rates within periphyton as the mats become more nutritious (Gaiser et al. 2011, Hagerthey et al. 2011). An increase in the oxidation of the periphyton substrate by bacterial assemblages within the mat is one theory explaining the breakdown of mats with P addition. McCormick et al. (2001) reported that periphyton ER rates tended to increase with P, although this response was not statistically significant. Similarly, we observed increased periphyton ER in SP compared with S treatments, but this effect was not significant. Our results suggest that salinity may be a stronger driver of altered periphyton mat structure than P in the southern Everglades where both elevated salinity and P simultaneously influence periphyton structure and taxonomic composition.

Compositional responses to salinity and phosphorus

Diatom species composition was significantly different between fresh and saltwater treated periphyton, as expected. However, aside from lower TC and AFDM in mats from salt compared with fresh treatments, periphyton functionality and chemistry (i.e., metabolism, nutrient and chl-a concentrations) were not significantly affected by elevated salinity. This suggests a level of functional redundancy in periphytic diatom communities along salinity gradients in the Everglades with different assemblages performing similar functions within the mats. It is important to keep in mind that only diatom responses were tested in this study even though periphyton includes other algal groups, as well as heterotrophic bacteria, that are extremely important to its functioning and structure. For example, CaCO₃-precipitating cyanobacteria or other mat-engineering species, which were not examined in this study, may have been lost in the elevated salinity treatment, which could explain the observed reduction in periphyton biomass in the S compared with F treatment. Interestingly, Mazzei et al. (2018) did not find functional redundancy in freshwater mats treated with monthly pulses of elevated salinity but rather reported reduced productivity, TC, TN, and TP as well as significant taxonomic differences between salt-treated and control plots. They attribute this to treating periphyton with monthly pulses, rather than continuous exposure, of elevated salinity, which may have allowed

the freshwater diatom assemblage to recover or prevent the establishment of salt-adapted species before the following monthly salt dosing. In this study, periphyton in the S treatments were continuously exposed to mean elevated salinity of 8 psu allowing a functionally redundant salt-tolerant diatom assemblage to become established. An important next step in unraveling periphyton responses to elevated salinity (and P), is to evaluate the effect of these drivers on the different biological components of the mats (e.g., cyanobacteria, green algae, and heterotrophic bacteria), using both morphological and molecular techniques.

No significant shifts in diatom composition were detected between F- and FP-treated mats, despite significantly greater mat TP concentrations in FP treatments. This supports our previous assumption that P inputs to FP mats were possibly adsorbed to CaCO₃ in the mats, making them biologically unavailable. Even though addition of P to freshwater mats did not result in a diatom assemblage shift, two species of *Gomphonema* and two species of *Nitzschia* were identified as indicators of enriched freshwater conditions, suggesting that even though overall assemblage dissimilarity was not significant a few individual species can still predict P loading into freshwater habitats. The absence of significant compositional changes in FP compared with F treatments may explain why no significant functional or chemical responses were detected with added P, other than elevated mat TP. On the other hand, periphyton from S and SP treatments did exhibit significant compositional dissimilarity as well as significant differences in functional and chemical parameters including elevated NEP, GPP, and TP in the SP compared with the S treatment. This suggests less functional redundancy in periphytic diatoms along P gradients in brackish habitats where composition shifts towards an assemblage of species that are more productive when P availability is greater, including *Amphora punctata*, *A. coffeaeformis aponina*, *Mastogloia braunii*, *Navicula salinicola*, and *Rhopalodia pacifica*. Identifying functional redundancy within ecological communities is important because, if present, it implies that using individual species or assemblages as bioindicators is a more powerful assessment method than measuring functional parameters as indicators of ecosystem change. Furthermore, if functional redundancy is absent within the community, species losses caused by changing environmental conditions can be expected to have strong impacts on ecosystem functioning.

CONCLUSIONS

Periphyton is regularly employed in ecosystem assessments of streams, lakes, and wetlands because of its ecological importance and sensitivity to environmental perturbation. In the Florida Everglades, periphyton is effectively used as an indicator of nutrient enrichment and hydrologic conditions and is major component of

ecosystem assessments and predictive models that inform management practices and policy. With increasing concern over the severity of saltwater intrusion into the Everglades, researchers have recognized the value of applying periphyton as a bioindicator of changes associated with sea-level rise in the coastal Everglades and are acting to develop periphyton metrics for early detection of the key environmental changes associated with it. This study contributes to the growing body of work aimed at understanding how the ecologically important calcareous, periphyton mats unique to karstic, freshwater wetlands respond to increased salinity and P availability caused saltwater intrusion. Saltwater intrusion is a major ecological and socio-economic concern for coastal, freshwater wetlands and left unresolved will inevitably result in the loss of these globally valuable ecosystems; however, the magnitude of its effects can be mitigated by employing predictive tools (e.g., periphyton and diatom metrics) to guide restoration projects aimed at repairing water connectivity and mitigating the landward push of coastal waters as sea level continues to rise. Future studies will focus on a complete evaluation of both heterotrophic and autotrophic taxonomic shifts in response to salinity and P, using a combination of morphological and molecular methods, to effectively capture the multifaceted responses of periphyton to saltwater intrusion.

ACKNOWLEDGMENTS

This research was supported by the National Science Foundation's Florida Coastal Everglades Long Term Ecological Research Program (DEB-1237517 and -1832229). Additional funding was provided through Florida Sea Grant R/C-S-56, including cooperative agreements with the South Florida Water Management District, the Everglades Foundation, and Everglades National Park. We are grateful to the State of Florida Department of Transportation Region 6 Office for working with us to gain permission to access and harvest peat for this experiment. We thank Laura Bauman, Rowan Johnson, Michael Kline, Michelle Robinson, and Ryan Stolee for help in the field; Andres Leon and Sara Osorio for help in sample processing and data entry; and Franco Tobias for laboratory assistance particularly with species identification. Viviana Mazzei was supported by the Florida International University Dissertation Year Fellowship and the Everglades Foundation For Everglades Fellowship. This is contribution number 920 from the Southeast Environmental Research Center in the Institute of Environment at Florida International University.

LITERATURE CITED

Affenzeller, M. J., A. Darehshouri, A. Andosch, C. Lütz, and U. Lütz-Meindl. 2009. Salt stress-induced cell death in the unicellular green alga *Micrasterias denticulata*. *Journal of Experimental Botany* 60:939–954.

Alam, S. M. 1999. Nutrient uptake by plants under stress conditions. Pages 285–313 in M. Pessarakli, editor. *Handbook of plant and crop stress*. CRC Press, Boca Raton, Florida, USA.

Azim, M. E., and T. Asaeda. 2005. Periphyton structure, diversity and colonization. Pages 15–35 in M. E. Azim, M. C. Verdegem, A. A. van Dam, and M. C. Beveridge, editors. *Periphyton: ecology, exploitation and management*. CABI Publishing, Cambridge, Massachusetts, USA.

Briceño, H., G. Miller, and S. E. Davis. 2014. Relating freshwater flow with estuarine water quality in the Southern Everglades mangrove ecotone. *Wetlands* 34:101–111.

Browder, J. A., P. J. Gleason, and D. R. Swift. 1994. Periphyton in the everglades: spatial variation, environmental correlates, and ecological implications. Pages 379–418 in S. E. Davis and J. C. Ogden. *Everglades: the ecosystem and its restoration*. St. Lucie Press, Boca Raton, Florida, USA.

Chambers, L. G., S. E. Davis, T. Troxler, J. N. Boyer, A. Downey-Wall, and L. J. Scinto. 2014. Biogeochemical effects of simulated sea level rise on carbon loss in an Everglades mangrove peat soil. *Hydrobiologia* 726:195–211.

Childers, D. L., J. N. Boyer, S. E. Davis, C. J. Madden, D. T. Rudnick, and F. H. Sklar. 2006. Relating precipitation and water management to nutrient concentrations in the oligotrophic “upside-down” estuaries of the Florida Everglades. *Limnology and Oceanography* 51:602–616.

Clarke, K. R., and R. N. Gorley, editors. 2006. *Primer v6: user manual/tutorial*. PRIMER-E, Plymouth, Massachusetts, USA.

Davis, S. M., D. L. Childers, J. J. Lorenz, H. R. Wanless, and T. E. Hopkins. 2005. A conceptual model of ecological interactions in the mangrove estuaries of the Florida Everglades. *Wetlands* 25:832–842.

De Cáceres, M. 2013. How to use the indicspecies package (ver. 1.7.1). R Proj 29. <https://cran.r-project.org/web/packages/indicspecies/vignettes/indicspeciesTutorial.pdf>

De Cáceres, M., P. Legendre, and M. Moretti. 2010. Improving indicator species analysis by combining groups of sites. *Oikos* 119:1674–1684.

Desrosiers, C., J. Leflaive, A. Eulin, and L. Ten-Hage. 2013. Bioindicators in marine waters: benthic diatoms as a tool to assess water quality from eutrophic to oligotrophic coastal ecosystems. *Ecological Indicators* 32:25–34.

Elser, J. J., M. E. Bracken, E. E. Cleland, D. S. Gruner, W. S. Harpole, H. Hillebrand, J. T. Ngai, E. W. Seabloom, J. B. Shurin, and J. E. Smith. 2007. Global analysis of nitrogen and phosphorus limitation of primary producers in freshwater, marine and terrestrial ecosystems. *Ecology Letters* 10:1135–1142.

Flower, H., M. Rains, D. Lewis, J. Z. Zhang, and R. Price. 2017. Saltwater intrusion as potential driver of phosphorus release from limestone bedrock in a coastal aquifer. *Estuarine, Coastal and Shelf Science* 184:166–176.

Gaiser, E. E. 2009. Periphyton as an indicator of restoration in the Florida Everglades. *Ecological Indicators* 9:37–45.

Gaiser, E. E., L. J. Scinto, J. H. Richards, K. Jayachandran, D. L. Childers, J. C. Trexler, and R. D. Jones. 2004. Phosphorus in periphyton mats provides the best metric for detecting low-level P enrichment in an oligotrophic wetland. *Water Research* 38:507–516.

Gaiser, E. E., J. C. Trexler, J. H. Richards, D. L. Childers, D. Lee, A. L. Edwards, L. J. Scinto, K. Jayachandran, G. B. Noe, and R. D. Jones. 2005. Cascading ecological effects of low-level phosphorus enrichment in the Florida Everglades. *Journal of Environmental Quality* 34:717–723.

Gaiser, E. E., J. C. Trexler, R. D. Jones, D. L. Childers, J. H. Richards, and L. J. Scinto. 2006. Periphyton responses to eutrophication in the Florida Everglades: cross-system patterns of structural and compositional change. *Limnology and Oceanography* 51:617–630.

Gaiser, E. E., J. M. L. Hée, F. A. Tobias, and A. H. Wachnicka. 2010. *Mastogloia smithii* var *lacustris* Grun.: a structural engineer of calcareous mats in karstic subtropical wetlands. *Proceedings of the Academy of Natural Sciences of Philadelphia* 160:99–112.

Gaiser, E. E., P. V. McCormick, S. E. Hagerthey, and A. D. Gottlieb. 2011. Landscape patterns of periphyton in the Florida Everglades. *Critical Reviews in Environmental Science and Technology* 41:92–120.

Hagerthey, S. E., B. J. Bellinger, K. Wheeler, M. Gantar, and E. E. Gaiser. 2011. Everglades periphyton: a biogeochemical perspective. *Critical Reviews in Environmental Science and Technology* 41:309–343.

Hasle, G. R., and G. A. Fryxell. 1970. Diatoms: cleaning and mounting for light and electron microscopy. *Transactions of the American Microscopical Society* 89:469–474.

Herbert, E. R., P. Boon, A. J. Burgin, S. C. Neubauer, R. B. Franklin, M. Ardon, K. N. Hopfensperger, L. P. M. Lamers, and P. Gell. 2015. A global perspective on wetland salinization: ecological consequences of a growing threat to freshwater wetlands. *Ecosphere* 6:1–43.

Hu, Y., and U. Schmidhalter. 2005. Drought and salinity: a comparison of their effects on mineral nutrition of plants. *Journal of Plant Nutrition and Soil Science* 168:541–549.

James, K. R., B. Cant, and T. Ryan. 2003. Responses of freshwater biota to rising salinity levels and implications for saline water management: a review. *Australian Journal of Botany* 51:703–713.

Johnson, R. E., N. C. Tuchman, and C. G. Peterson. 1997. Changes in the vertical microdistribution of diatoms within a developing periphyton mat. *Journal of the North American Benthological Society* 16:503–519.

La Hée, J. M., and E. E. Gaiser. 2012. Benthic diatom assemblages as indicators of water quality in the Everglades and three tropical karstic wetlands. *Freshwater Science* 31:205–221.

Lee, S. S., E. E. Gaiser, B. Van De Vijver, M. B. Edlund, and S. A. Spaulding. 2014. Morphology and typification of *Mastogloia smithii* and *M. lacustris*, with descriptions of two new species from the Florida Everglades and the Caribbean region. *Diatom Research* 29:325–350.

Lee, D., B. J. Wilson, S. Servais, V. Mazzei, and J. Kominoski. 2019. The Salinity and phosphorus mesocosm experiment in freshwater sawgrass wetlands: Determining the trajectory and capacity of freshwater wetland ecosystems to recover carbon losses from saltwater intrusion (FCE LTER), Florida, USA from 2015 to 2018. Environmental Data Initiative. <https://doi.org/10.6073/pasta/a269722318964f74cb5cabf87f0d3fb3>. Dataset accessed 11/14/2019.

Lu, C., and A. Vonshak. 2002. Effects of salinity stress on photosystem II function in cyanobacterial *Spirulina platensis* cells. *Physiologia Plantarum* 114:405–413.

Mazzei, V., and E. E. Gaiser. 2018. Diatoms as tools for inferring ecotone boundaries in a coastal freshwater wetland threatened by saltwater intrusion. *Ecological Indicators* 88:190–204.

Mazzei, V., et al. 2018. Functional and compositional responses of periphyton mats to simulated saltwater intrusion in the southern Everglades. *Estuaries and Coasts* 41:2105–2119.

McCormick, P. V., and M. B. O'Dell. 1996. Quantifying periphyton responses to phosphorus in the Florida Everglades: a synoptic-experimental approach. *Journal of the North American Benthological Society* 15:450–468.

McCormick, P. V., and R. J. Stevenson. 1998. Periphyton as a tool for ecological assessment and management in the Florida Everglades. *Journal of Phycology* 34:726–733.

McCormick, P. V., M. B. O'Dell, R. B. Shuford, J. G. Backus, and W. C. Kennedy. 2001. Periphyton responses to experimental phosphorus enrichment in a subtropical wetland. *Aquatic Botany* 71:119–139.

McCormick, P. V., J. W. Harvey, and E. S. Crawford. 2011. Influence of changing water sources and mineral chemistry on the Everglades ecosystem. *Critical Reviews in Environmental Science and Technology* 41:28–63.

McVoy, C. W., W. P. Said, J. Obeysekera, J. Van Arman, and T. W. Dreschel. 2011. *Landscapes and hydrology of the predrainage everglades*. University of Florida Press, Gainesville, Florida, USA.

Mendelssohn, I. A., and D. P. Batzer. 2006. Abiotic constraints for wetland plants and animals. Pages 82–114 in D. P. Batzer and R. R. Sharitz, editors. *Ecology of freshwater and estuarine wetlands*. University of California Press, Berkeley, California, USA.

Odum, E. P., J. T. Finn, and E. H. Franz. 1979. Perturbation theory and the subsidy-stress gradient. *BioScience* 29:349–352.

Pan, Y., R. J. Stevenson, P. Vaithianathan, J. Slate, and C. J. Richardson. 2000. Changes in algal assemblages along observed and experimental phosphorus gradients in a subtropical wetland, USA. *Freshwater Biology* 44:339–353.

Potapova, M., and D. F. Charles. 2007. Diatom metrics for monitoring eutrophication in rivers of the United States. *Ecological Indicators* 7:48–70.

Price, R. M., P. K. Swart, and J. W. Fourqurean. 2006. Coastal groundwater discharge—an additional source of phosphorus for the oligotrophic wetlands of the Everglades. *Hydrobiologia* 569:23–36.

R Core Team. 2017. R version 3.3.3. R Project for Statistical Computing, Vienna, Austria. www.R-project.org

Rejmánková, E., and J. Komárová. 2000. A function of cyanobacterial mats in phosphorus-limited tropical wetlands. *Hydrobiologia* 431:135–153.

Rejmánková, E., and K. Komárová. 2005. Response of cyanobacterial mats to nutrient and salinity changes. *Aquatic Botany* 83:87–107.

Richardson, C. J., and S. S. Qian. 1999. Long-term phosphorus assimilative capacity in freshwater wetlands: a new paradigm for sustaining ecosystem structure and function. *Environmental Science & Technology* 33:1545–1551.

Ross, M. S., J. F. Meeder, J. P. Sah, P. L. Ruiz, and G. J. Telewski. 2000. The Southeast Saline Everglades revisited: a half-century of coastal vegetation change. *Journal of Vegetation Science* 11:101–112.

Saha, A. K., S. Saha, J. Sadle, J. Jiang, M. S. Ross, R. M. Price, L. S. Sternberg, and K. S. Wendelberger. 2011. Sea level rise and South Florida coastal forests. *Climatic Change* 107:81–108.

Schedlbauer, J. L., J. W. Munyon, S. F. Oberbauer, E. E. Gaiser, and G. Starr. 2012. Controls on ecosystem carbon dioxide exchange in short-and long-hydroperiod Florida Everglades freshwater marshes. *Wetlands* 32:801–812.

Scinto, L. J., and K. R. Reddy. 2003. Biotic and abiotic uptake of phosphorus by periphyton in a subtropical freshwater wetland. *Aquatic Botany* 77:203–222.

Servais, S., J. S. Kominoski, S. P. Charles, E. E. Gaiser, V. Mazzei, T. G. Troxler, and B. J. Wilson. 2019. Saltwater intrusion and soil carbon loss: testing effects of salinity and phosphorus loading on microbial functions in experimental freshwater wetlands. *Geoderma* 337:1291–1300.

Stevenson, J. 2014. Ecological assessments with algae: a review and synthesis. *Journal of Phycology* 50:437–461.

Solórzano, L., and J. H. Sharp. 1980. Determination of total dissolved phosphorus and particulate phosphorus in natural waters 1. *Limnology and Oceanography* 25:754–758.

Stevenson, R. J., Y. Pan, and H. van Dam. 1999. *Assessing environmental conditions in rivers and streams with diatoms in The diatoms: applications for the environmental and earth sciences*. Second edition. Cambridge University Press, Cambridge, UK.

Sudhir, P., and S. D. S. Murthy. 2004. Effects of salt stress on basic processes of photosynthesis. *Photosynthetica* 42:481–486.

Taffs, K. H., K. M. Saunders, and B. Logan. 2017. Diatoms as indicators of environmental change in estuaries. Pages 277–294 in K. Weckström, K. M. Saunders, P. A. Gell, and C. G. Skilbeck, editors. Applications of paleoenvironmental techniques to estuarine systems. Developments in paleoenvironmental research. Springer, Dordrecht, The Netherlands.

Touchette, B. W. 2007. Seagrass-salinity interactions: physiological mechanisms used by submersed marine angiosperms for a life at sea. *Journal of Experimental Marine Biology and Ecology* 350:194–215.

Trexler, J. C., E. E. Gaiser, J. S. Kominoski, and J. Sanchez. 2015. The role of periphyton mats in consumer community structure and function in calcareous wetlands: lessons from the Everglades. Pages 155–170 in J. A. Entry, A. D. Gottlieb, K. Jayachandran, and A. Ogram, editors. *Microbiology of the everglades ecosystem*. CRC Press, Boca Raton, Florida, USA.

Trobajo, R., L. Rovira, D. G. Mann, and E. J. Cox. 2011. Effects of salinity on growth and on valve morphology of five estuarine diatoms. *Phycological Research* 59:83–90.

Troxler, T. G., D. L. Childers, and C. J. Madden. 2014. Drivers of decadal-scale change in southern Everglades wetland macrophyte communities of the coastal ecotone. *Wetlands* 34:81–90.

Vymazal, J., and C. J. Richardson. 1995. Species composition, biomass, and nutrient content of periphyton in the Florida Everglades. *Journal of Phycology* 31:343–354.

Weston, N. B., M. A. Vile, S. C. Neubauer, and D. J. Velinsky. 2011. Accelerated microbial organic matter mineralization following salt-water intrusion into tidal freshwater marsh soils. *Biogeochemistry* 102:135–151.

Williams, A. A., N. T. Lauer, and C. T. Hackney. 2014. Soil phosphorus dynamics and saltwater intrusion in a Florida estuary. *Wetlands* 34:535–544.

Wilson, B. J., S. Servais, S. P. Charles, V. Mazzei, E. E. Gaiser, J. S. Kominoski, J. H. Richards, and T. G. Troxler. 2019. Phosphorus alleviation of salinity stress: effects of saltwater intrusion on an Everglades freshwater peat marsh. *Ecology* 100: e02672.

Xue, S. K. 2018. Appendix 3A-5: Water year 2017 and five-year (water year 2012–2017) annual flows and total phosphorus loads and concentrations by structure and area. In 2018 South Florida Environmental Report—Volume I. South Florida Water Management District, West Palm Beach, Florida, USA.

SUPPORTING INFORMATION

Additional supporting information may be found online at: <http://onlinelibrary.wiley.com/doi/10.1002/eap.2067/full>

DATA AVAILABILITY

Data are available on the LTER Network Data Portal: <https://doi.org/10.6073/pasta/a269722318964f74cb5cabf87f0d3fb3>